AFRL-AFOSR-VA-TR-2021-0017

Large-Scale Terahertz Systems: Sub-wavelength Field and Sub-picosecond Temporal Control for Programmable Terahertz Generation

Kaushik Sengupta
TRUSTEES OF PRINCETON UNIVERSITY
1 NASSAU HALL
PRINCETON, NJ,
US

02/19/2021
Final Technical Report

Air Force Research Laboratory
Air Force Office of Scientific Research
Arlington, Virginia 22203
Air Force Materiel Command

REPORT DOCUMENTATION PAGE

Form Approved
OMB No. 0704-0188

1. REPORT DATE *(DD-MM-YYYY)*	**2. REPORT TYPE**	**3. DATES COVERED** *(From - To)*
19-02-2021	Final	01 Jul 2019 - 30 Jun 2020

4. TITLE AND SUBTITLE
Large-Scale Terahertz Systems: Sub-wavelength Field and Sub-picosecond Temporal Control for Programmable Terahertz Generation

5a. CONTRACT NUMBER

5b. GRANT NUMBER
FA9550-19-1-0316

5c. PROGRAM ELEMENT NUMBER

6. AUTHOR(S)
Kaushik Sengupta

5d. PROJECT NUMBER

5e. TASK NUMBER

5f. WORK UNIT NUMBER

7. PERFORMING ORGANIZATION NAME(S) AND ADDRESS(ES)
TRUSTEES OF PRINCETON UNIVERSITY
1 NASSAU HALL
PRINCETON, NJ
US

8. PERFORMING ORGANIZATION REPORT NUMBER

9. SPONSORING/MONITORING AGENCY NAME(S) AND ADDRESS(ES)
AF Office of Scientific Research
875 N. Randolph St. Room 3112
Arlington, VA 22203

10. SPONSOR/MONITOR'S ACRONYM(S)
AFRL/AFOSR RTA1

11. SPONSOR/MONITOR'S REPORT NUMBER(S)
AFRL-AFOSR-VA-TR-2021-0017

12. DISTRIBUTION/AVAILABILITY STATEMENT
A Distribution Unlimited: PB Public Release

13. SUPPLEMENTARY NOTES

14. ABSTRACT
Power generation in the terahertz spectrum has been notoriously challenging due to the limited performance of solid-state materials and devices at these frequencies. While there has been a surge of research work in the past decade focusing on closing the THz gap with efficient chip-scale systems, there still remains a considerable challenge to generate tens of mW of power in the 0.3-1.0 THz range. The overall goal of this project was to investigate new methods of nonlinear synchronization across multiple sources to enable large scale sources to enable beamforming and high power generation at Terahertz, and to allow such systems to enable 2D localization among multiple moving nodes.
In this work,
1) We proposed a new method to create time-synchronization across THz oscillator arrays establishing a robust frequency and phase distribution across the entire chip for high power THz generation. We demonstrate the scalable nature of this approach with 4x4 array and spatially combine radiated power. The chip generates a radiated power of -3 dBm with an EIRP of +14 dBm at 416 GHz in a lensless setup using a 65 nm CMOS process. We experimentally demonstrate the beamforming of 30 degrees in both E and H plane. This is the highest EIRP array demonstrated at these frequencies enabled through the mechanism of the scalable synchronization techniques.
2) We demonstrate THz PRISM, a spectrum-to-space mapping methodology to allow simultaneous one-shot localization of multiple mobile wireless nodes with dispersive THz beams across 360-400 GHz.

15. SUBJECT TERMS

16. SECURITY CLASSIFICATION OF:			**17. LIMITATION OF ABSTRACT**	**18. NUMBER OF PAGES**	**19a. NAME OF RESPONSIBLE PERSON**
a. REPORT	**b. ABSTRACT**	**c. THIS PAGE**			KENNETH GORETTA
U	U	U	UU	20	**19b. TELEPHONE NUMBER** *(Include area code)* 426-7349

AFOSR Final Report: Large-Scale Terahertz Systems: Sub-wavelength Field and Sub-picosecond Temporal Control for Programmable Terahertz Generation

AFOSR Grant # FA9550-19-1-0316

Kaushik Sengupta (PI) Electrical Engineering

kaushiks@princeton.edu

Princeton University

1.1 Summary:

Power generation in the terahertz spectrum has been notoriously challenging due to the limited performance of solid-state materials and devices at these frequencies. While there has been a surge of research work in the past decade focusing on closing the THz gap with efficient chip-scale systems, there still remains a considerable challenge to generate tens of mW of power in the 0.3-1.0 THz range. The overall goal of this project was to investigate new methods of nonlinear synchronization across multiple sources to enable large scale sources to enable beamforming and high power generation at Terahertz, and to allow such systems to enable 2D localization among multiple moving nodes.

In this work,

1) We proposed a new method to create time-synchronization across THz oscillator arrays establishing a robust frequency and phase distribution across the entire chip for high power THz generation. We demonstrate the scalable nature of this approach with 4x4 array and spatially combine radiated power. The chip generates a radiated power of -3 dBm with an EIRP of +14 dBm at 416 GHz in a lensless setup using a 65 nm CMOS process. We experimentally demonstrate the beamforming of 30 degrees in both E and H plane. ***This is the highest EIRP array demonstrated at these frequencies enabled through the mechanism of the scalable synchronization techniques.***

2) We demonstrate ***THz PRISM, a spectrum-to-space mapping methodology to allow simultaneous one-shot localization of multiple mobile wireless nodes with dispersive THz beams across 360-400 GHz.***

Publications (flagship journals and peer-reviewed flagship conferences) and Patents:

2020: *IEEE International Solid-State Circuits Conference (ISSCC), flagship conference in solid-state circuits and silicon chips*
2021: *IEEE International Solid-State Circuits Conference (ISSCC), flagship conference in solid-state circuits and silicon chips*
2021: IEEE Journal of Solid State Circuits (2 papers in preparation), *flagship journal in solid-state circuits and silicon chips*

[1] H.Saeidi, S.Venkatesh, X.Lu, and K.Sengupta, ``THz Prism: One-Shot Simultaneous Multi-Node Angular Localization Using Spectrum-to-Space Mapping with 360-to-400GHz Broadband Transceiver and Dual-Port Integrated Leaky-Wave Antennas," *IEEE International Solid-state Circuits Conf. (ISSCC)*, Feb. 2021.

[2] H. Saeidi, S. Venkatesh, C. R. Chappidi, T. Sharma, C. Zhu, and K. Sengupta, ``A 4x4 Distributed Multi-Layer Oscillator Network for Harmonic Injection and THz Beamforming with 14dBm EIRP at 416GHz in a Lensless 65nm CMOS IC" *IEEE International Solid-state Circuits Conf. (ISSCC)*, San Francisco, Feb. 2020.

[3] H. Saeidi, S. Venkatesh, C. R. Chappidi, T. Sharma, C. Zhu, and K. Sengupta, ``Scalable THz Phased Array with nonlinear coupled synchronization network " *IEEE Journal Solid-State Circuits (JSSCC) (in preparation)*.

[4] H.Saeidi, S.Venkatesh, X.Lu, and K.Sengupta, ``THz Prism: Rapid and one-Shot Localization with THz spectrum-to-space Mapping," *IEEE Journal Solid-State Circuits (JSSCC) (in preparation)*.

Awards:

- PI selected as the IEEE Microwave Theory and Techniques Distinguished Lecturer, 2020-2021.
- PI selected as the IEEE Solid-State Circuits Society Distinguished Lecturer, 2019-2020.
- Hooman Saeidi awarded Analog Devices Outstanding Student Designer Award in 2020.

Student supported: Hooman Saeidi (currently fourth year graduate student)

Patents:

- A provisional patent will be filed on the THz PRISM localization technology for simultaneous finding of multiple mobile wireless nodes.

Talks:

- Distinguished Lecture in IEEE Solid State Circuits Society, Oregon, Dec.2020.
- Distinguished Lecture in IEEE Solid State Circuits Society, IIT Gandhinagar, Dec. 2020
- IEEE MTT and IEEE Photonics co-sponsored talk at IIT BHU, Oct. 2020
- ACM Nanocomm, Sept 2020.
- Global Foundry 6G CTC, Aug. 2020.
- IEEE International Workshop on Terahertz Communications, May 2020.
- SRC/Qualcomm Decadal Workshop, Qualcomm, San Diego, Feb. 2020.
- IEEE Microwave Theory and Techniques, Webinar Series, Nov. 2019.
- Rice University, Solid-State Circuits Distinguished Lecture, Houston, Nov. 2019.
- International Photonics and Optoelectronics Meeting (POEM), Wuhan, China, Nov. 2019.
- Plenary speaker, International Workshop on THz Technologies, Delhi, Sep. 2019.
- SPIE Photonics and Terahertz, San Diego, Aug. 2019.

2.1: THz Phased Array and Large-scale Nonlinear Synchronization for Beamforming

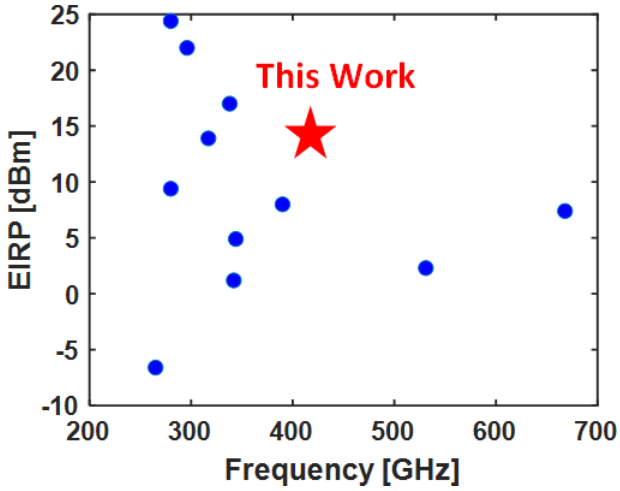

Fig. 1. Overview of the state-of-the-art integrated coherent sources in silicon.

In this work, we demonstrate

1) A new method to enable large-scale synchronization among multiple THz sources for the highest EIRP and beamforming at 420 GHz.
2) The highest silicon-integrated THz array with highest EIRP at 420 GHz

Synchronizing THz sources that individually generate small power to generate large power quasi-optically can allow not only high power beams but also electronically controlled beamforming. Such multiple harmonic sources require low loss coupling mechanisms which are robust to process, voltage, and temperature (PVT) variations. Coupling mechanisms often involve lossy transmission lines and at THz frequencies, such passive networks suffer from low quality factors and thus limit scalability, power generation capability, and programmability of the overall system. Hence, achieving coupling mechanisms at lower frequency and boosting the coherent signals to higher frequencies is an attractive alternative option. However, such a mechanism is extremely power hungry and requires robust low-loss design of LO-distribution layer which can be extremely challenging in terms of scalable implementation. In this article, we take a novel approach to design a robust, coupled oscillator network with high locking range. ***We used a 2D oscillating network with negative Gm (-Gm) cells at each node that do not oscillate individually but only collectively, establishing a robust frequency and phase distribution network across the chip for high THz power generation. T***he key idea here is to convert the network that sustains oscillation into the network that accomplished nonlinear synchronization (Fig. 3). This allows scalability into large arrays with various geometries to allow scalable THz power generation (Fig. 4).

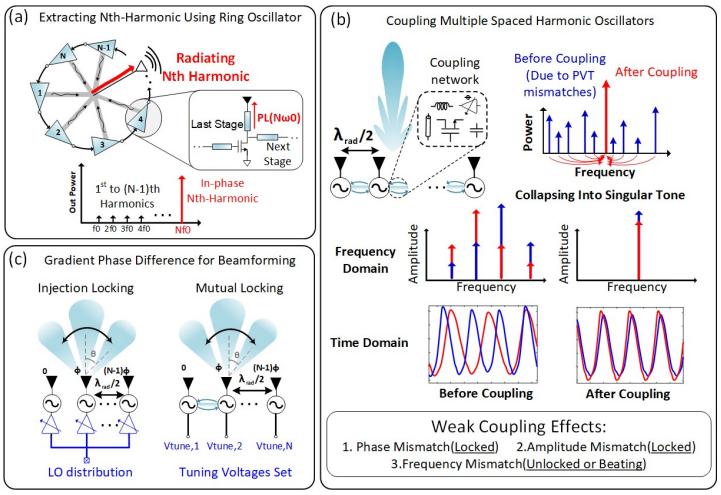

Fig. 2. Design approaches for scalable integrated terahertz power generation using *fmax* limited devices with beam forming capability. (a) Extracting and radiating Nth harmonic from the N-Stage Ring-oscillator, while canceling 1^{st} to $(N\ 1)^{th}$ Harmonic (b) Coupling Multiple $\lambda/2$ spaced oscillators using active and passive devices to overcome PVT mismatches. Weak coupling will result in phase and amplitude mismatch between the sources. (c) Beam forming by injecting LO signals with phase gradient to the injection-locked oscillators or varying the resonance frequency of the mutually locked sources that result in the phase difference between them.

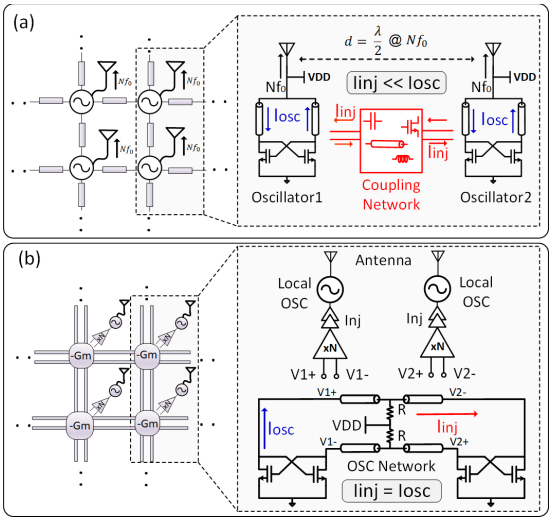

Fig. 3. (a) Conventional design of scalable coupled oscillators. In these designs the injection current is lower than the oscillator current which result in the limited, low locking range. (b) Proposed multi-layer oscillator network. In the first layer of this network, -Gm cells will behave as a single oscillator.

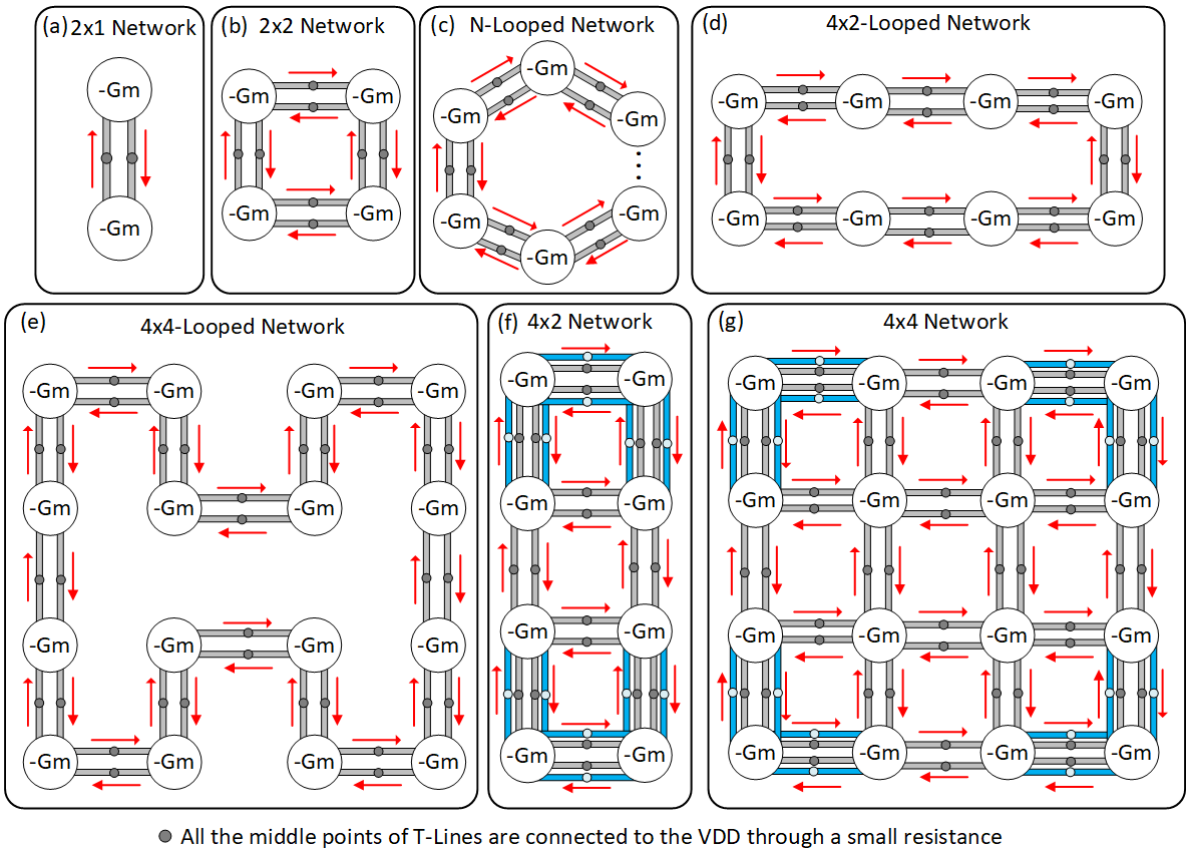

Fig. 4. Different scalability approaches in coupled oscillator networks. (a) – (e) Shows the flow in scaling up the oscillator network in which the –Gm cells will not cause oscillation individually, but only collectively. In these set of network, each cell is connected to two neighboring –Gm cells. (f),(g): In these set of scalable oscillators network, each –Gm cell is connected to 4 neighboring cells. Extra transmission lines are added to equalize the loading the cells across the network.

The next obvious step is to first scale this locking mechanism stage to larger networks to achieve: 1) higher coherent power outputs beamforming/beam-steering with phase gradients (phased arrays). With 2x1 dual-core network as the basic building block, one can scale this network to a 2x2 -Looped, 4x2- Looped, and 4x4-Looped networks as shown in Figs.4 b-e respectively. This scheme can be scaled to a 2D network to establish a robust frequency reference across the chip at 69.3 GHz (Fig 4). It can be observed from Fig. 4, that the corner, edge and center cells see a different number of neighboring elements. To allow equal loading on all cells, we employ 4 differential t-lines across the corner and edge cells as shown in Fig 4. To synthesize harmonic signals above f_{max}, the output of each –Gm cell interfaces with a frequency doubler (139 GHz), which in turn injection locks to a local 3-stage harmonically optimized ring oscillator (Fig. 5). The output signal at 416 GHz is radiated out with an on-chip patch antenna. To allow beamforming, we need to establish a phase gradient across the array. While the oscillating

network limits the phase variations at f_0 (69.3 GHz), the phase gradient at the radiating harmonic frequency of 416 GHz can still be substantial. This is achieved with varactor tuning in each –Gm cell that allows beamforming capability without sacrificing robustness in locking, as shown in Fig. 5. The simulated radiation efficiency of the antenna is 47%. The simulated power from each cell is -10.5 dBm at 416 GHz for a total simulated output power of -2 dBm and an EIRP of 15 dBm.

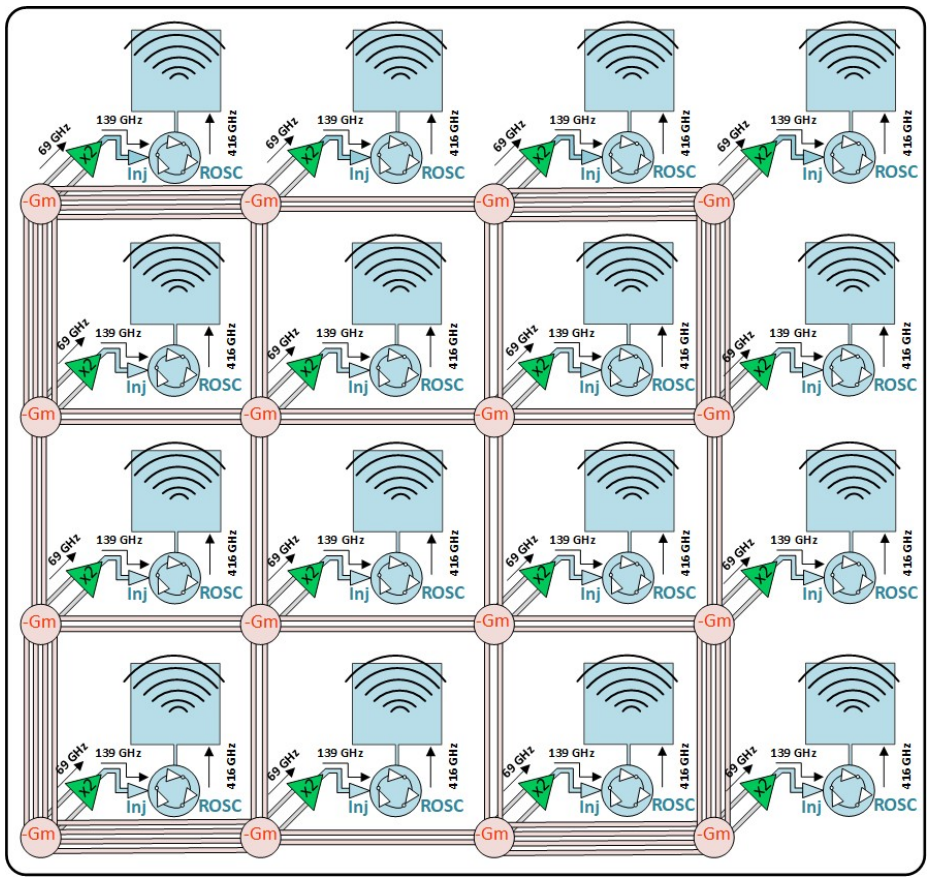

Fig. 5. Multi-layer oscillator circuit architecture. In this design, first layer consists of 4×4 –Gm cells resulting in the oscillation frequency off0= 69.3GHz. This frequency is then locally doubled and injected into ring oscillators with the fundamental frequency of 138.6 GHz and the signal with the frequencyof6f0= 416 GHz is extracted and radiated through a microstrip patch antenna.

The chip is fabricated in 65 nm CMOS process (Fig. 6). The measured peak EIRP is +14 dBm at 416 GHz and varying between 5-14 dBm across 412-419 GHz with identical varactor tuning.

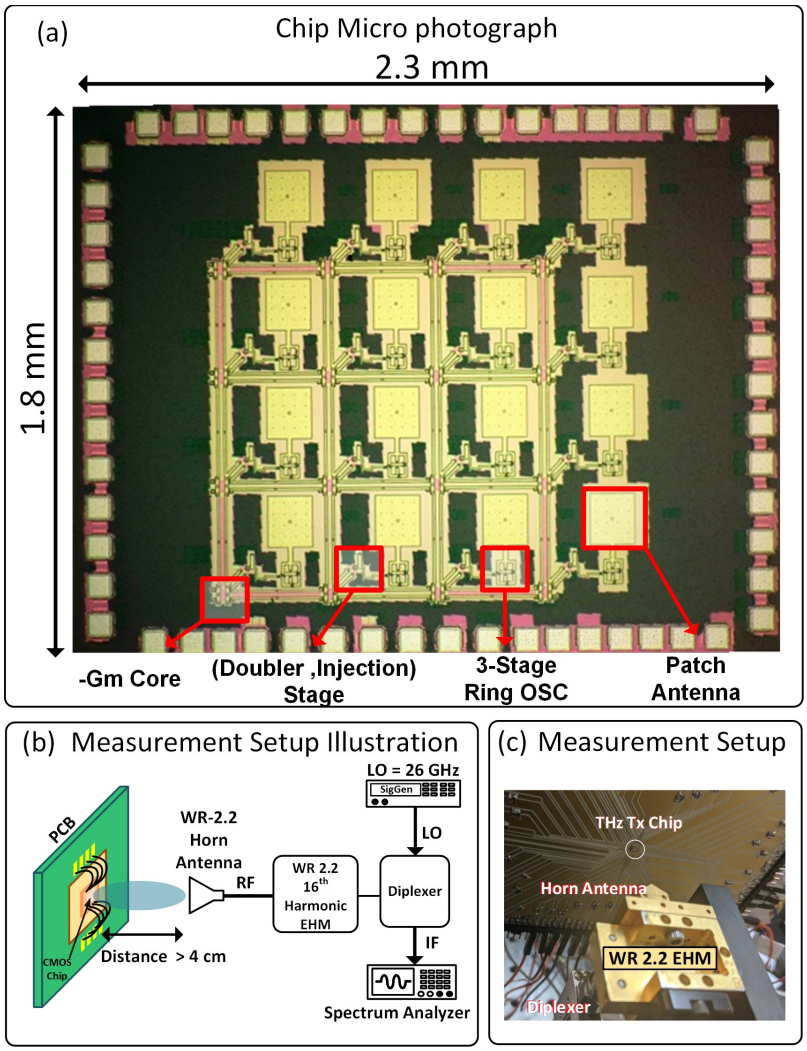

Fig 6. (a) Chip microphotograph. (b) Measurement setup. (c) Photographof the measurement setup

The method to create phased surface on the chip to allow THz beamforming rests on the nonlinear synchronization in this complex 2D network. Fig. 7 shows the nonlinear optimization method that we follow to create the phase gradient on the surface. Fig. 8 shows the simulated phase gradient as a result of the varactor programmability and the measured THz beamforming.

This is the highest Effective-isotropic-radiated-power generated in a silicon chip without a lens at 416 GHz with the simultaneous ability to allow beamforming.

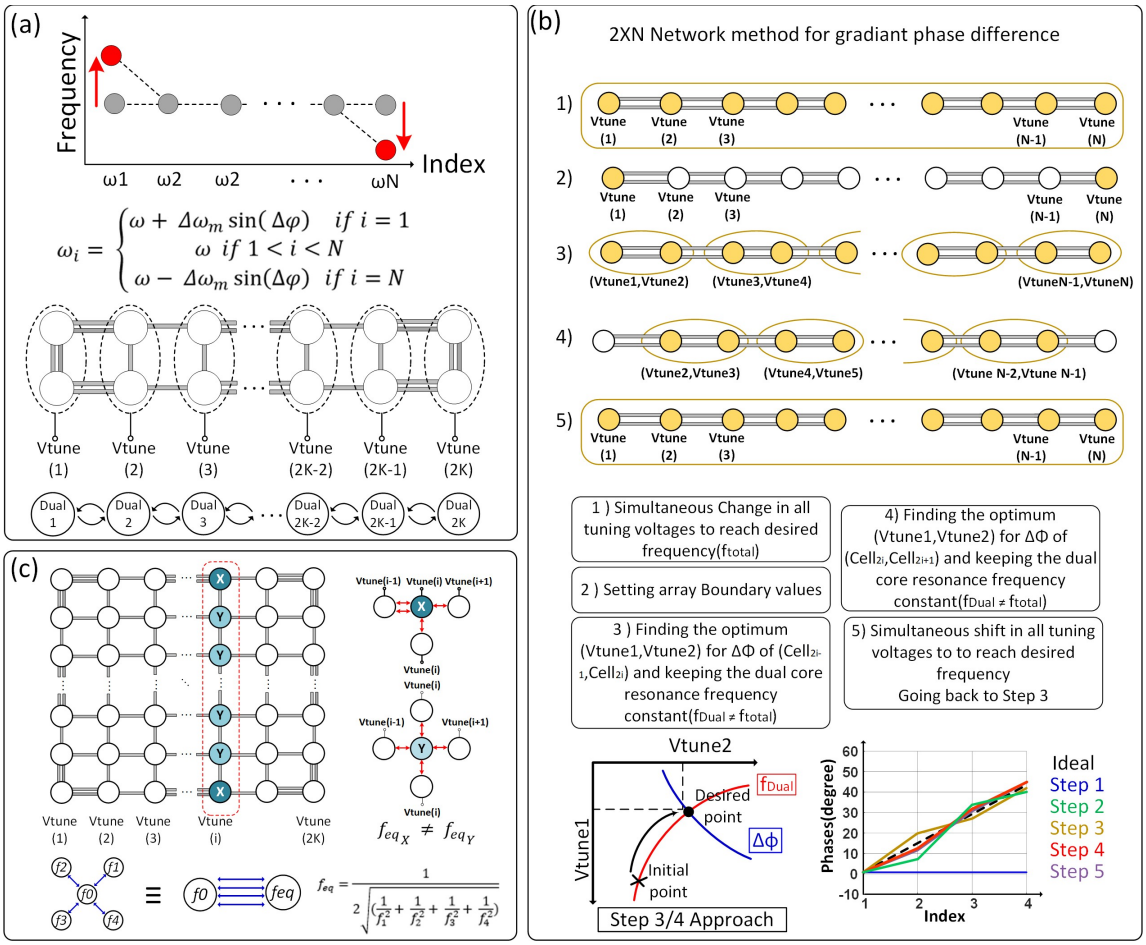

Fig. 7. (a) Technique to create gradient phase difference in a 1D array of mutually locked oscillators. (b) Iterative algorithm towards creating a phasedifference 2×N oscillator network. In 2×N network of oscillators, each dual-core is considered as a single oscillator. (c) Different resonance frequency ofthe cells in each column while having the same tuning voltages as the effect of the difference in their neighboring cells

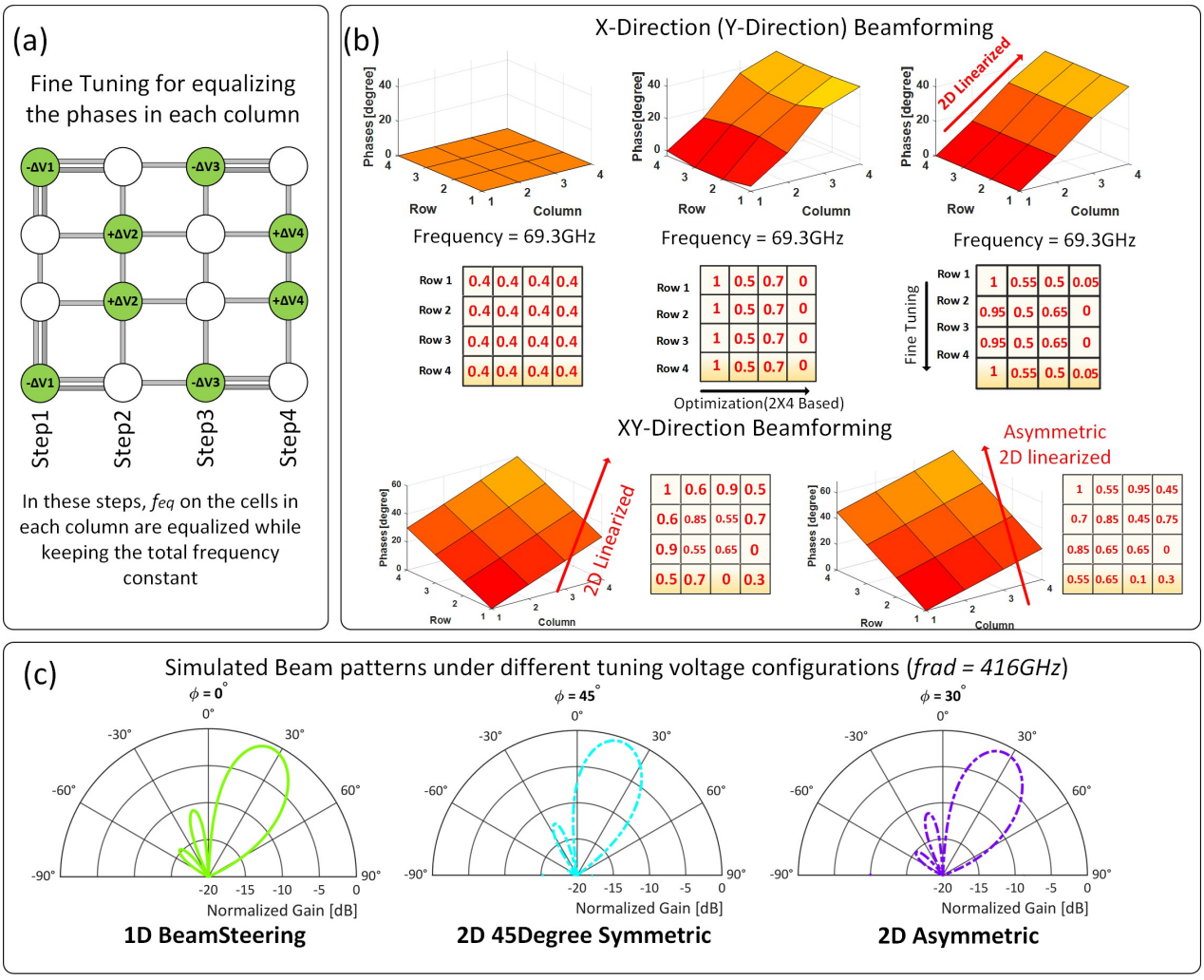

Fig. 8. (a) Fine voltage tuning to equalize the phases in each column while keeping the overall radiated frequency constant. (b) The tuning voltages at the1st layer of the multi-layer oscillator network for 1D and 2D beamforming. (c) Simulated beam patterns under different tuning voltage configurations for 2Dbeamforming.

2.2 THz Prism: One-shot Simultaneous Multi-node Angular Localization using Spectrum-to-Space Mapping with 360-400 GHz Broadband Transceiver and Dual-port Integrated Leaky Wave Antennas

The spectrum above 100 GHz is expected to spawn a generation of ultra-high-speed wireless links and intelligent sensing and imaging applications. They are expected to be supported through a heterogeneous and dynamically reconfigurable wireless network fabric in 5G and beyond. Such wireless communication and sensing applications require rapid localization and direction finding of mobile nodes. This functionality is paramount for communications-on-the-move applications, wireless link discovery, rapid beam alignment/ tracking at mmWave and THz frequencies. The current protocols for direction finding and beam alignment in 5G mmWave systems are based on iterative algorithms which are often non-scalable, time-consuming, and computationally expensive thus posing serious challenges for low latency applications. Thus there is a need to process such direction-finding methods at the 'edge nodes', to enable secure scalable networks with very low latencies. In this article, we present a spectrum-to-space mapping principle, where localization information can be processed at the edge 'sensor node' through spectrum sensing. The conceptual idea is presented in Fig.9 that shows an access point (transmitter/receiver) that acts as a THz prism casting different spectral portions of a broadband THz signal across space. If the mapping is unique, multiple edge nodes can simultaneously localize themselves in a single shot fashion through localized spectrum sensing, avoiding the use of the slow iterative process and bi-directional communication. In this paper, we present a scalable 360-400GHz transceiver architecture in 65-nm CMOS with frequency-dependent beam synthesis using two dual-port integrated frequency-dispersive leaky-wave radiators. The two antennas when excited/sensed across the two opposite end-ports cover a 1D spatial angle across $\pm 40^{O}$, and enable 2D localization with two such ICs covering both orthogonal basis vectors with a frequency offset radiation (Fig.9). Exploiting the cross-correlation of the spectrum-to-space mapping (Fig. 9), the system achieves 2D localization accuracy of $\sigma_{\varphi} = 1.9^{o}$ and $\sigma_{\Theta} = 1.95^{o}$ for a measurement time of 50ms.

The architecture of the chip is shown in Fig. 10. The chip consists of two leaky wave antennas (LWA) whose two ends are fed by on-chip broadband signal synthesis and reception capability across 360-400GHz. The off-chip LO signal across 59–71 GHz is converted into a differential on-chip signal, and amplified by 3-stage differential power amplifiers (PA). The PA has a simulated gain of 19.9dB, with Psat of 15.52dBm and a peak PAE of 25.9%. The amplified differential signal is then fed to a doubler across 108-142GHz followed by an on-chip balun and a tripler stage. The combination of the doubler-tripler generates a measured peak power of -10.9dBm across 360-400GHz. The single-ended output of the tripler is then impedance matched and fed to the LWA. Exploiting a 20dB isolation between the two ends of the antennas, the other

ports of the two LWAs are integrated with a 360-400GHz Rx. For the Rx, the output of the antenna is first converted to differential signal through a rat race balun followed by a double balanced passive mixer. The LO to the mixer is generated in a similar manner as that of the Tx chain. The IF output of the mixer is then fed to an IF amplifier with a simulated gain of 16dB with a bandwidth of 15GHz. The passive mixer has an overall double sideband Rx noise figure (NF) of 18.1dB.

To allow unique spectrum-to-space mapping, we avoid the use of multi-frequency MIMO array by exploiting the frequency-dependent beam-pointing abilities of frequency-diverse surfaces. In this work, we employ two compact, moderate gain, wide-band, on-chip LWA. When a broadband pulse or a chirp is injected into such an antenna, the lower part of the spectrum radiates along the broadside and the higher part in an end-fire fashion (Fig.9). This feature is exploited to create a frequency-dependent spatial map response, which forms the basis vector to enable spatial localization of the mobile wireless nodes. By computationally analyzing a single spectral response from an unknown wireless link, one can enable link discovery techniques in a fast and effective manner without the need for scanning or mapping the 2D space. Dual on-chip LWAs enable 1D hemispherical coverage of the space. Further, two such orthogonally placed chips potentially enable 2D hemispherical coverage.

The design of the on-chip 360-400GHz LWA is shown in Fig. 11. The on-chip LWA antenna consists of a periodic slot array with a spacing of 43μm and an overall length of 1.7mm. LWA waveguide width is chosen to be 225 μm which corresponds to TE(1,0) mode cut-off frequency of 320GHz. The LWA width, length, and the periodic slot spacing govern the dispersion relationship and support only positive propagating vectors thereby covering the positive quadrant of the hemisphere. Though one could design the LWA to support the negative propagating vectors (composite left-handed material), these are extremely susceptible to losses. To cover the other quadrant, we enable another LWA which is fed from the opposite end with another dedicated Tx. The simulated maximum gain of the LWA is 4.5dBi at 378GHz with a radiation efficiency of 19.3%. The LWA has fan-beam radiation patterns, with lower frequencies pointing close to broadside and higher frequencies to 40O. The LWA supports linear polarization and is oriented parallel to the direction of periodic slots. Exploiting a ~20dB isolation of the two LWA end-ports, a single antenna is interfaced with a Tx and an Rx at its two ends. Therefore, each IC can be configured to support three different modes of operation for link discovery, namely: transmitter only mode, receiver only mode, and full-duplex transceiver mode covering a frequency range of 360-400GHz. The measured radiation patterns and the frequency-dependent beam maxima in Fig. 11 demonstrates the key principle behind the proposed direction finding. The measured co-to-cross polarization ratio is about ~18dB and the measured EIRP of the transmitter at 378GHz is -6.4dBm. The complete Rx chain average NF (including the antenna) is measured to be ~26.2dB across the operating band. (Fig. 11).

To enable 1D direction-of-arrival (DOA) estimation, spectrum to angular map is shown in Fig. 12, which captures the frequency-dependent radiation patterns (Fig. 11). Since the system is deterministic, given a spectrum from an unknown angle, we perform a correlation with this map and estimate the values that maximize the correlation. The number of frequency samples required to determine the basis calibration map is determined by the dispersion curve of the LWA as shown in Fig.11. We show the angle of arrival error as a function of measurement time (resolution bandwidth) of the IF sampled signal. As shown in Fig.12, the system along with our algorithm has a DoA estimation error of 0.95O for measurement time of 5ms. With faster localization at 50µs, the DoA estimation error is about 2.1O. Measurements are performed using WR9.0 signal generation extension (SGX) followed by a WR4.3 frequency doubler and a WR2.2 second harmonic mixer which acts as an external Tx or Rx.

We also perform 2D DoA estimation using two orthogonal Tx chips transmitting slightly different frequencies (1kHz offset). Similar to 1D localization, we create 2D frequency-to-space calibration maps that allow to perform 2D localization. We show the measured error in angle estimation and corresponding θ and φ error in Fig.13. The measured 2D angle accuracy is $\sigma_{\varphi} = 1.9^{o}$ and $\sigma_{\Theta} = 1.95^{o}$ for a measurement time of 50ms. The functionality of 1D DoA estimation is also demonstrated between a Tx and an Rx enabled chip and is also shown in Fig.13. The comparison table in Fig. 14 demonstrates the state of the art performance.

In summary, we demonstrate for the first Terahertz spectrum-to-space mapping for rapid and simultaneous localization of multiple mobile nodes with fully integrated THz transceivers and frequency-dispersive radiators.

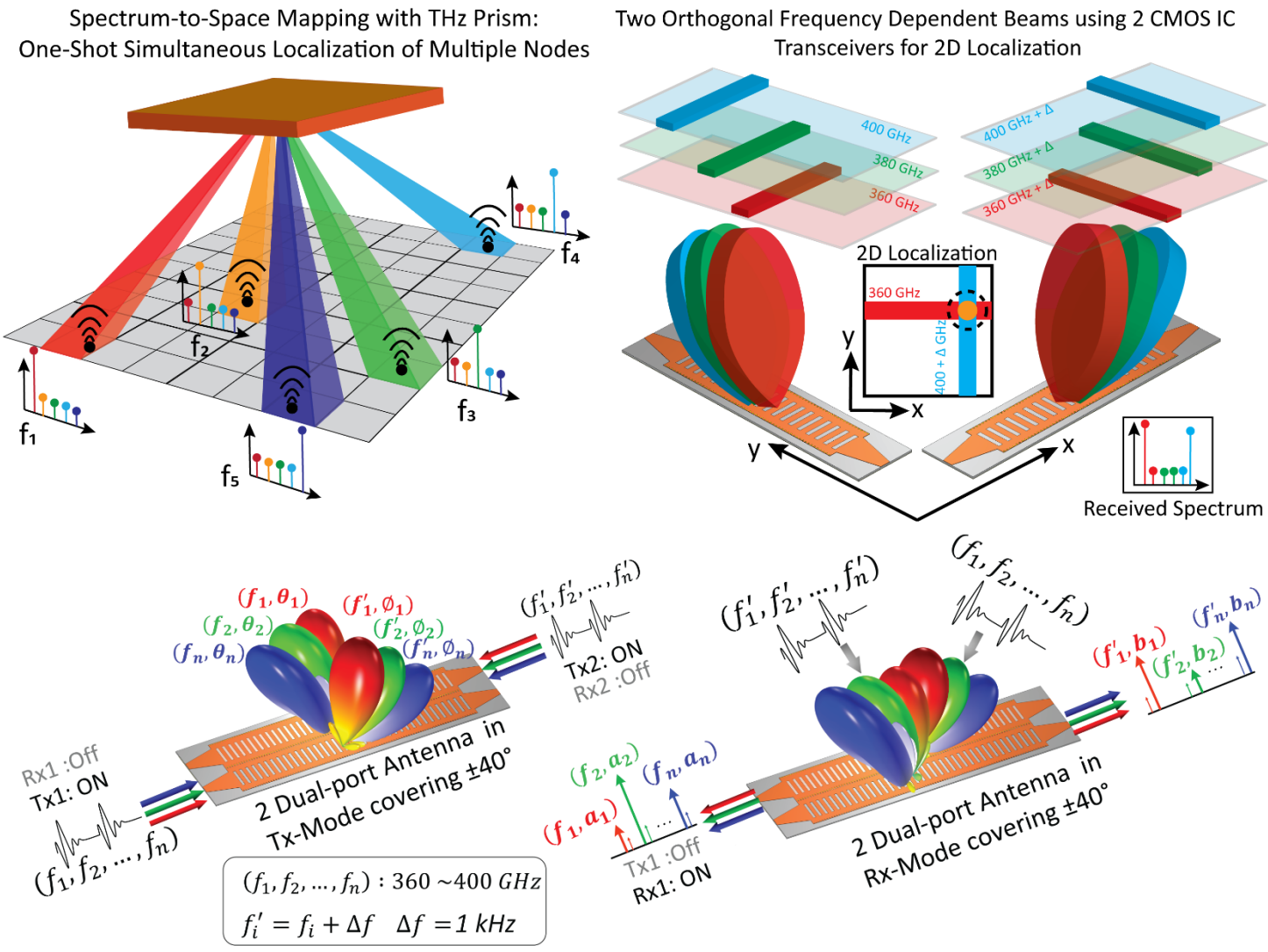

Fig 9. Concept of Spectrum-to-Space mapping with THz Prism. Simultaneous and one-shot detection of multiple wireless nodes using frequency diverse radiators is shown. Implementaion of THz prism using two orthogonally placed leaky wave radiators with integrated transceivers for 2D localization of wireless nodes. Two dual port antennas with opposite feed points are deployed to cover +/- 40°.

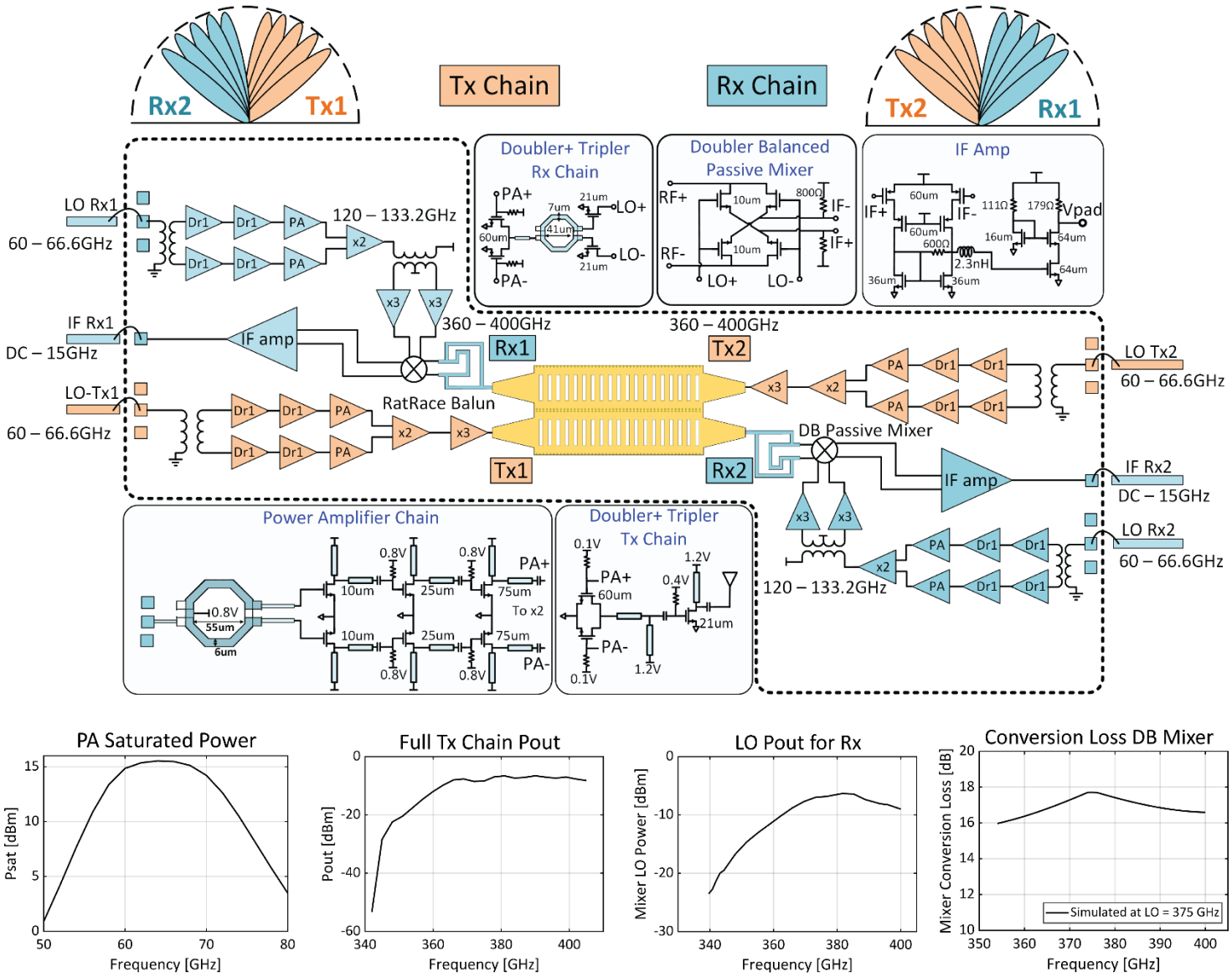

Fig 10. Broadband 360- 400 GHz transceiver archiecture with two dual port on chip LWAs. The chip consists of 2 Tx and 2 Rx to cover the top hemisphere of +/- 40° for localization. Simulation results of the on chip PA, full Tx chain output power, LO chain output power and the double-balanced mixer conversion loss are shown.

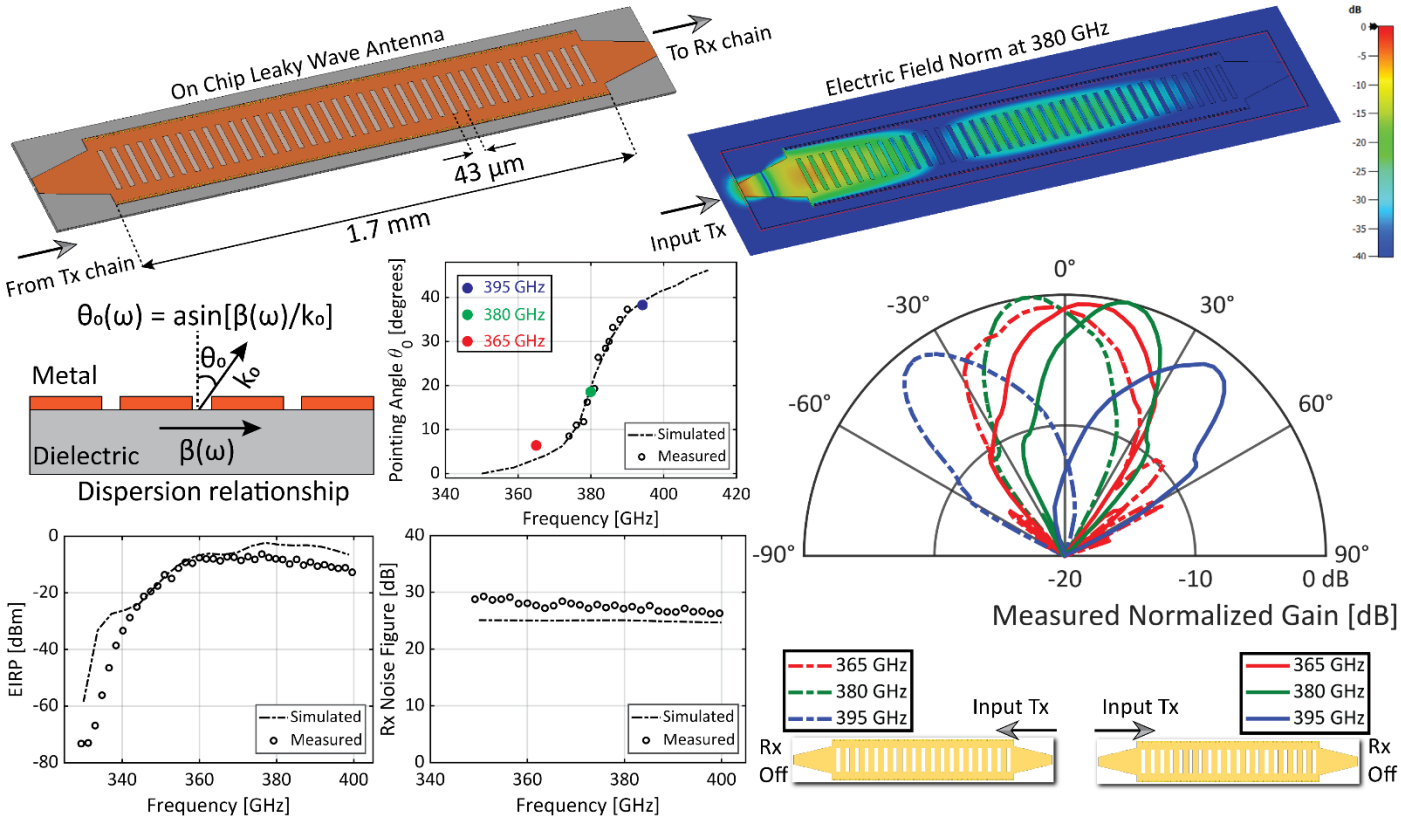

Fig 11. Leaky wave antenna design and Tx/Rx characterizations. The figure shows the electric field strength decays as the wave propagates through the leaky wave structure at 380 GHz. Measured antenna beam patterns are shown for two on chip Txs excited from opposite directions. Beam pointing locations vary from broadside to +40° when excited from left (shown in solid lines) and vary from broadside to -40° when excited from right (shown in dashed lines). The simulated and measured frequency versus pointing angles are also shown and follows a particular dispersion relationship as mentioned in the equation. The simulated and measured EIRP and noise figure of the Tx and Rx respectively are also plotted.

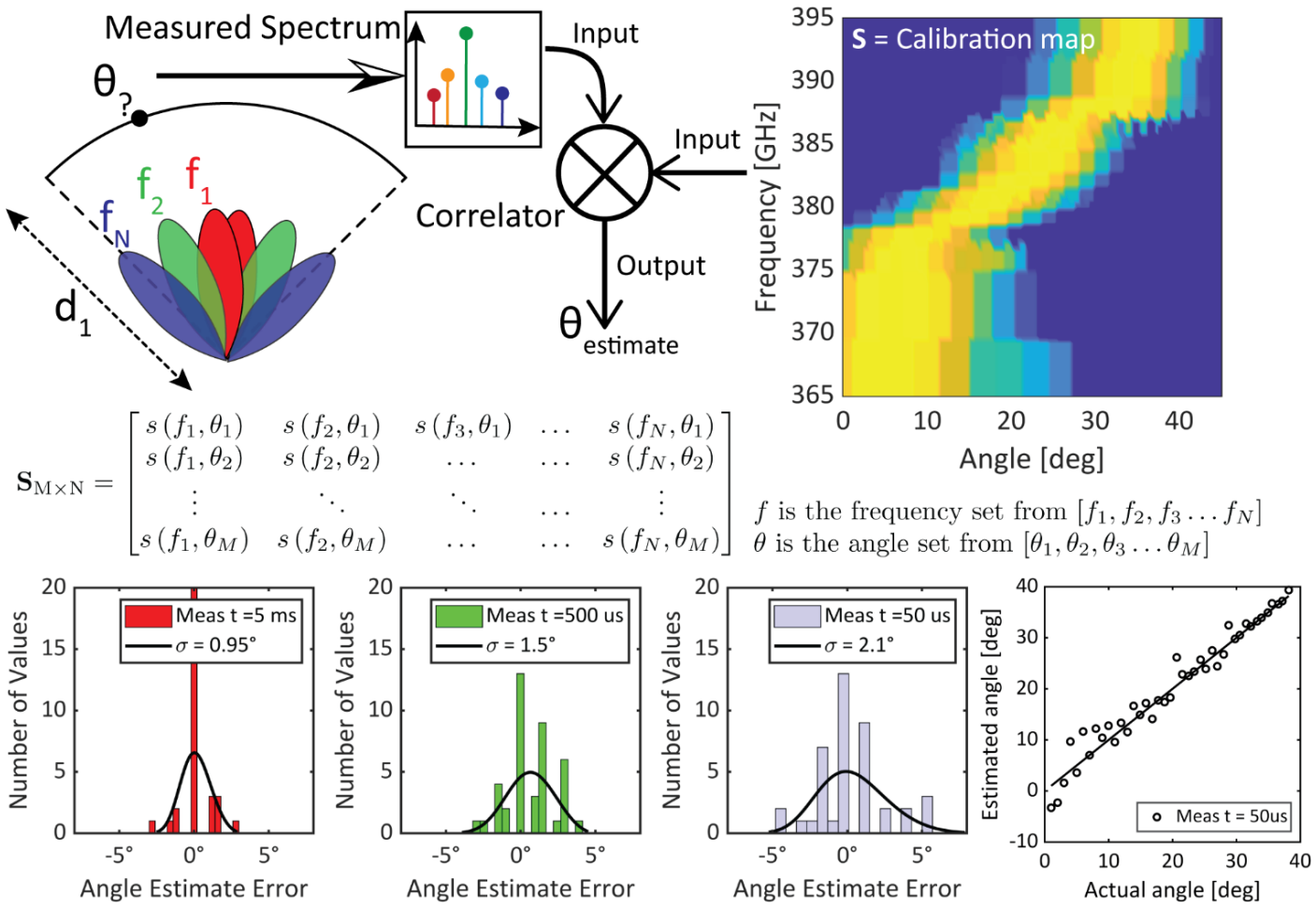

Fig 12. Concept and measurement performance of 1D angular localization using one CMOS IC. The antenna response as a function of frequency versus angle is initially mapped to form the basis calibration matrix S. As shown in the figure, localization is performed exploiting cross-correlation of the measured spectrum against this calibration matrix S. The estimated angle and the standard deviations are shown for different measurement times for randomized node locations.

.

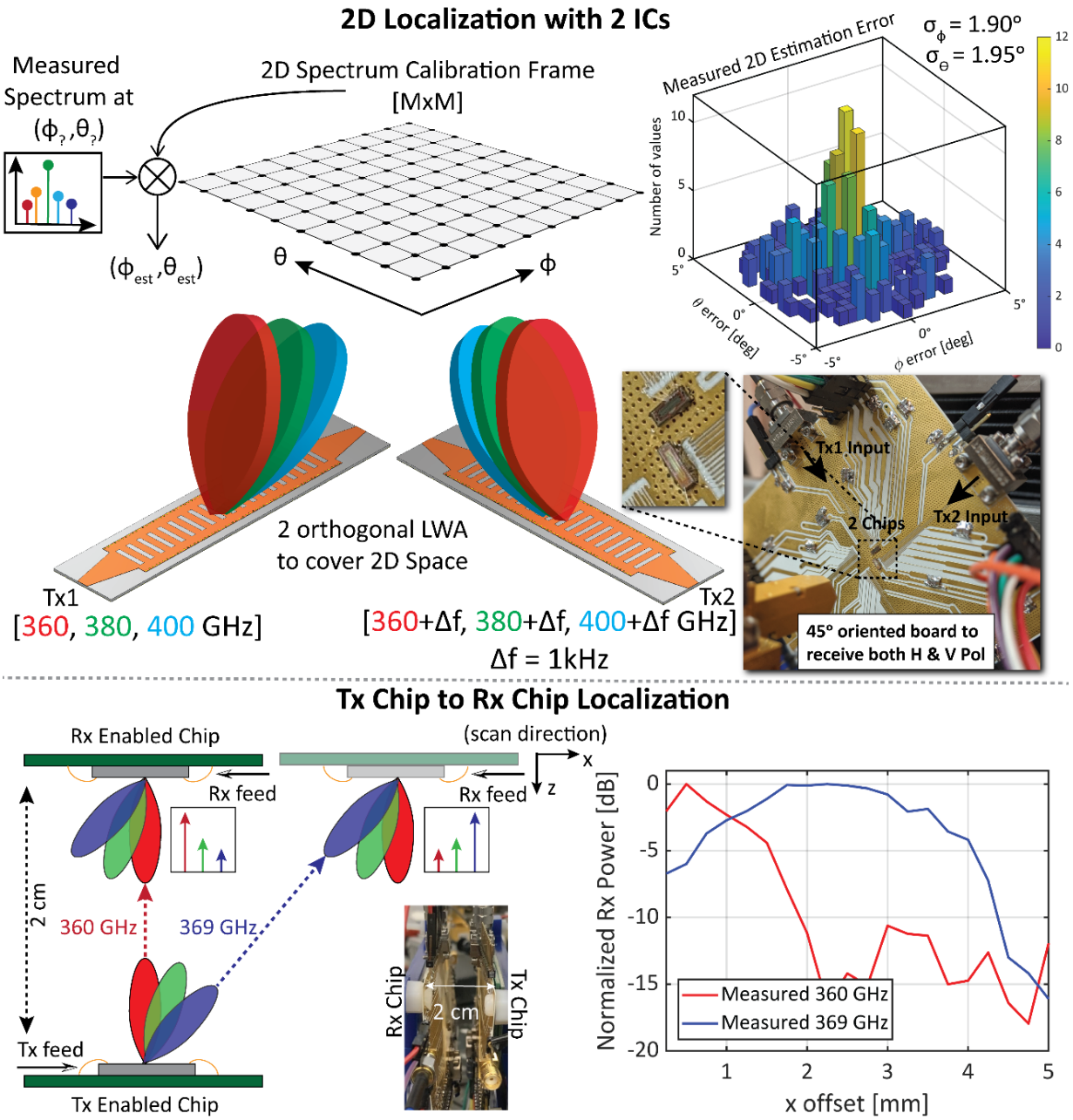

Fig. 13 Localization concept with two orthogonally placed chips. The overall measurement error statistics demonstrate 2D angular error of 1.9° and 1.95° in the two orthogonal axis. The figure also shows the experimental setup where the two orthogonal Tx chips are placed 45° with respect to the external receiver. The figure also shows a chip to chip localization capability using two separate Tx and Rx enabled chips placed at a distance of 2cm.

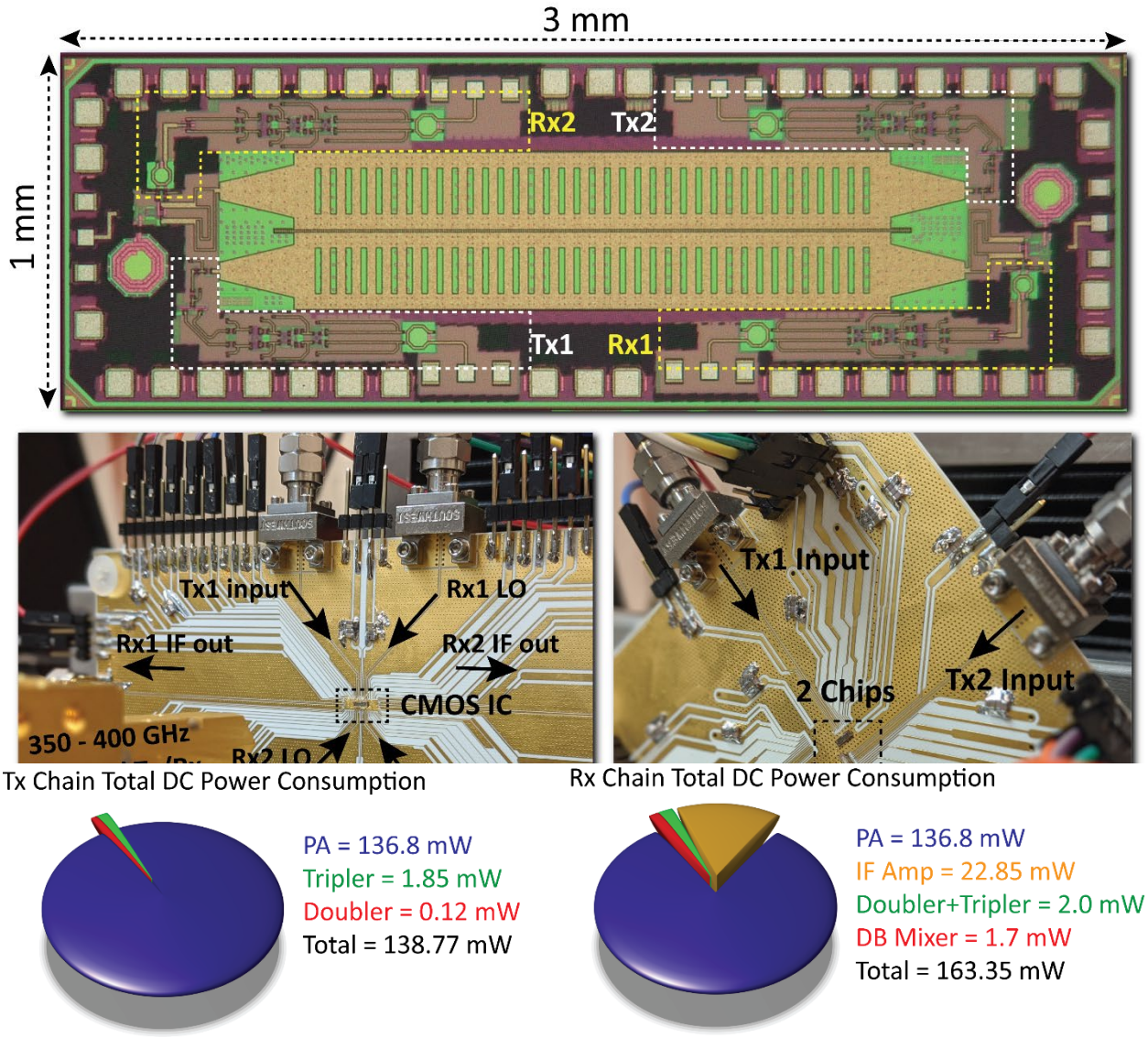

Fig 14. Fabricated chip photograph and experimental setups.

Summary:

In this project, we demonstrated a nonlinear dynamical approach to enabling large-scale high power THz phased arrays and a new method for simultaneous and one-shot localization of multiple wireless nodes with spectrum-to-space mapping with THz beams. In the first work, we demonstrated the highest EIRP silicon-based THz source with +14 dBm EIRP at 416 GHz with 2D beamforming capability. In the second work, we demonstrated 2D angular localization with 360-400 GHz integrated dispersive radiators and fully integrated THz transceivers. Both of these works were presented in the flagship conference in solid-state circuits and silicon chips, IEEE ISSCC and two journal papers are in preparation for these works.

[1] H.Saeidi, S.Venkatesh, X.Lu, and K.Sengupta, ``THz Prism: One-Shot Simultaneous Multi-Node Angular Localization Using Spectrum-to-Space Mapping with 360-to-400GHz Broadband Transceiver and Dual-Port Integrated Leaky-Wave Antennas," *IEEE International Solid-state Circuits Conf. (ISSCC)*, Feb. 2021.

[2] H. Saeidi, S. Venkatesh, C. R. Chappidi, T. Sharma, C. Zhu, and K. Sengupta, ``A 4x4 Distributed Multi-Layer Oscillator Network for Harmonic Injection and THz Beamforming with 14dBm EIRP at 416GHz in a Lensless 65nm CMOS IC" *IEEE International Solid-state Circuits Conf. (ISSCC)*, San Francisco, Feb. 2020.

[3] H. Saeidi, S. Venkatesh, C. R. Chappidi, T. Sharma, C. Zhu, and K. Sengupta, ``Scalable THz Phased Array with nonlinear coupled synchronization network " *IEEE Journal Solid-State Circuits (JSSCC) (in preparation)*.

[4] H.Saeidi, S.Venkatesh, X.Lu, and K.Sengupta, ``THz Prism: Rapid and one-Shot Localization with THz spectrum-to-space Mapping," *IEEE Journal Solid-State Circuits (JSSCC) (in preparation)*.